Spring 2021

Purification and Functional Characterization of the Iron-Responsive Transcription Factor Aft1 from C. glabrata

Jade Ikahihifo-Bender
University of South Carolina - Columbia

PURIFICATION AND FUNCTIONAL CHARACTERIZATION OF THE IRON-RESPONSIVE TRANSCRIPTION FACTOR AFT1 FROM *C. GLABRATA*

By

Jade Ikahihifo-Bender

Submitted in Partial Fulfillment
of the Requirements for
Graduation with Honors from the
South Carolina Honors College

May 2021

Approved:

Caryn E. Outten

Caryn Outten
Director of Thesis

Angela-Nadia Albetel

Angela-Nadia Albetel
Second Reader

Steve Lynn, Dean
For South Carolina Honors College

TABLE OF CONTENTS

SUMMARY

Iron is utilized as a co-factor for many biological processes and is also a key factor during fungal infections as the human host and invading pathogens battle over limited iron pools. The primary iron-responsive transcription factor Aft1 in the opportunistic pathogenic yeast *Candida glabrata* responds to iron deficiency by activating expression of iron acquisition genes. However, the mechanisms for sensing intracellular iron levels and regulating Aft1 activity are unknown. This study aims to delineate these essential iron regulation pathways by overexpressing and purifying recombinant Aft1 and three potential iron-sulfur cluster binding partners, Grx3, Grx4, and Bol2, so that the mechanism for regulating Aft1 activity in response to iron may be characterized.

ABSTRACT

Due to its unique ability to serve as both an electron donor and acceptor, iron is utilized as a co-factor for many biological processes, including electron transfer, oxygen binding, and vitamin synthesis. Iron is also a key factor during fungal infections as the human host and invading pathogens battle over limited iron pools. The primary iron-responsive transcription factor Aft1 in the opportunistic pathogenic yeast *Candida glabrata* responds to iron deficiency by activating expression of iron acquisition genes. However, the mechanisms for sensing intracellular iron levels and regulating Aft1 activity in response to iron are unknown. The *C. glabrata* iron regulation system shares close homology to a similar system in the non-pathogenic yeast *Saccharomyces cerevisiae,* in which the monothiol glutaredoxins Grx3/4 and the BolA-like protein Bol2 form [2Fe-2S] binding complexes that deactivate Aft1 under iron replete conditions. To determine whether a similar mechanism controls *C. glabrata* Aft1 activity, we sought to analyze the *in vitro* interactions between Grx3, Grx4, and Bol2 from this yeast pathogen. For this project, we successfully subcloned the *AFT1, GRX3, GRX4,* and *BOL2* genes from *C. glabrata* into *Escherichia coli* overexpression vectors allowing for expression of recombinant Aft1 and its presumed binding partners Grx3/4 and Bol2 alone or in complex. The overexpression conditions identified here will be used to purify these target proteins and characterize their structure and iron regulation function. In accordance with this aim, Aft1 and Grx4 were purified, and a fluorescence polarization assay was used to measure the DNA binding affinity of Aft1.

INTRODUCTION

Iron is an essential nutrient that supports many cellular processes such as oxidative phosphorylation and metabolism, cellular growth and proliferation, and the transport and storage of gaseous signaling molecules.[1,2] Maintenance of optimal intracellular iron levels is critical, as both iron deficiency and iron overload are detrimental to human health.[1] In fact, iron deficiency is the most common nutritional deficiency in the world affecting over one billion people, and iron overload disorders are among the most common autosomal recessive disorders in Caucasian populations.[1,2] Iron levels in the body are also a target for opportunistic pathogens that compete with the human host.[3] An immune-compromised individual with disrupted iron sequestration would be less competitive for iron and thus subject to the virulence of an opportunistic pathogen.[3] *Candida glabrata*, for example, is an opportunistic pathogen commonly found in healthy mucosa that is the second leading cause of candidemia, a potentially lethal fungal infection in the bloodstream.[3]

Our lab has used the non-pathogenic fungi *Saccharomyces cerevisiae* (baker's yeast) in experiments that study the structure,

function, and subcellular localization of iron binding proteins involved in iron trafficking and regulation.[4-6] In this organism, the iron-responsive transcription factors Aft1 and Aft2 activate iron uptake genes in iron deplete conditions.[4,7] The genes activated by Aft1/2 are required for the acquisition and high affinity import of ionic iron and siderophore-bound iron from the environment when intracellular iron levels are low. The Aft1/2 regulators are deactivated under iron replete conditions by binding an iron-sulfur (Fe-S) cluster to prevent iron overload.[4,7] The cytosolic proteins Grx3/4 and Bol2 facilitate binding between the Fe-S cluster and Aft1/2.[4]

Studies utilizing this model system have delineated mechanisms that are essential to regulating iron homeostasis in a non-pathogenic yeast.[4-7] The pathogenic yeast *C. glabrata* presumably employs a similar iron regulatory system as *S. cerevisiae*;[8] however, little is known regarding the molecular mechanisms of iron regulation in this pathogen. Extending iron binding protein studies to *C. glabrata* is necessary to characterize the iron regulation pathways that are essential to its virulence.[3] Our lab aims to address this by overexpressing and purifying recombinant Aft1, Grx3/4, and Bol2, so that the functional interactions of Aft1 with target genes and potential binding partners may be characterized. Aft1 involvement in iron regulation in *C. glabrata* is essential for the virulence of this pathogen,[8] so these findings will improve understanding of how iron regulation impacts human susceptibility to fungal infections and have implications for the development of prophylactic or therapeutic treatments for fungal infections.

MATERIALS AND METHODS

Plasmid Construction

The pET21a vector (Novagen) for expression of recombinant proteins in *Escherichia coli* confers ampicillin resistance and contains a *lac*O promoter driving protein expression that is inducible by the addition of isopropyl β-D-thiogalactosidase (IPTG). The *AFT1* gene from *C. glabrata* was inserted into this vector creating a C-terminal 6xHis-tagged Aft1 (Aft1-6xHis referred to as Aft1 throughout). The corresponding plasmid was named pET21a-Aft1-6xHis or pEA100. The pRSFDuet-1 vector (Novagen) for co-expression of multiple recombinant proteins in *E. coli* confers kanamycin resistance and also contains an IPTG-inducible *lac*O promoter. This vector was used to insert Grx3 or Grx4 and Bol2 from *C. glabrata* alone and in tandem resulting in plasmids named pRSFDuet-1-Grx4 or pEA102, pRSFDuet-1-Bol2 or pEA103, pRSFDuet-1-Grx4-Bol2 or pEA104, pRSFDuet-1-Grx3 or pEA105, and pRSFDuet-1-Grx3-Bol2 or pEA106.

To assemble a plasmid containing the gene of interest in its respective vector backbone, the gene of interest was amplified from 10 ng, 25 ng, or 50 ng of *C. glabrata* genomic DNA (ATCC) by polymerase chain reaction (PCR) using forward and reverse primers (Table 1, Eurofins Genomics). To allow for ligation of the target sequence into the vector backbones, the forward primer incorporated a restriction enzyme site before the start codon, and the reverse primer incorporated a restriction enzyme site after the stop codon (Table 1).

PCR reactions included 10 µL 5X Q5 Reaction Buffer, 10 mM dNTPs, 10 µM forward primer, 10 µM reverse primer, 0.5 µL Q5 High-Fidelity DNA Polymerase (New England Biolabs), 10 µL 5X Q5 High GC Enhancer, and nuclease-free water to 25 µL. The reactions were performed with 30 cycles of melting temperature 98 °C for 10 s, respective annealing temperature for 30 s, and extension temperature 72 °C according to the 25 s/kb amplification rate of Q5 High-Fidelity DNA Polymerase (Table 2).

Table 1: Primers used and restriction enzyme sites incorporated for amplifying target genes from *C. glabrata* genome and cloning into *E. coli* expression vectors.

Primer Name	Primer Sequence (5' to 3')[a,b,c]	Enzyme Site
Aft1 FOR	tttaagaaggagatata**catATG**GATTCCAACCAACTAATAC	*Nde*I
Aft1 REV	cagtggtggtggtggtggtg**ctcgag**CATTATGTGATCTTCTTCTAATTTAAC	*Xho*I
Grx4 FOR	catcaccacagcca**ggatcc**ATGGAGGGGGGAAGGAGG	*Bam*HI-HF
Grx4 REV	cattatgcggccgc**aagctt**CTAGTTATTTACTCGTATGGTGTGTTGG	*Hind*III-HF
Bol2 FOR	ctgacgtcggtaccc**tcgag**ATGATTACTGAAGAACATCTG	*Xho*I
Bol2 REV	ggcagcagcctagg**ttaattaa**TTAAATTACTATCTTTGACCACTC	*Pac*I
Grx3 FOR	accatcatcaccacagcca**ggatcc**ATGTCTGTTGTTGATATAGATAATG	*Bam*HI-HF
Grx3 REV	ttaagcattatgcggccgc**aagctt**TTACAGTGATAACTTCTTGTTAAAG	*Hind*III-HF

[a]Lower-case nucleotides align with the vector backbones.
[b]Upper-case nucleotides align with the gene of interest.
[c]Restriction sites used for cloning the gene of interest are in **bold**.

Table 2: Annealing temperatures and extension times used in PCR for each construct.

Plasmid	Annealing Temp (°C)	Insert Size (bp)	Extension Time (s)
pEA100	58.0	1651	50
pEA102	65.5	823	25
pEA103/ pEA104	57.3	297	25
pEA105/ pEA106	58.2	779	25

PCR products were confirmed via agarose gel electrophoresis and combined for purification with the Wizard® SV Gel and PCR Clean-Up System (Promega) protocol. The purified DNA fragment was cloned into its corresponding vector backbone to generate a plasmid via double digestion with the restriction enzymes corresponding to the sites incorporated during cloning (Table 1, Thermo Fisher Scientific) in CutSmart NEBuffer (New England Biolabs). The vector backbone (1 µg) was incubated with the enzymes at 37 °C for 1 h to generate overlapping ends for annealing with the target gene; the reactions were further incubated according to NEB recommendations to inactivate the enzymes. The HiFi Assembly (HA) protocol (New England Biolabs) was used to ligate the DNA insert into the digested vector backbone through incubation for 15 or 30 min at 50 °C. The assembled constructs were confirmed with 0.8-1% agarose gel electrophoresis.

E. coli Transformation

The confirmed plasmids were transformed into *E. coli* DH5α cells. Cultures were plated on Luria Bertani (LB) media supplemented with 100 µg/mL ampicillin (Amp) for pEA100 and 60 µg/mL kanamycin (Kan) for pEA102-106 and incubated at 37 °C overnight. Colonies were grown overnight in 5 mL LB-Amp or LB-Kan media. Plasmid DNA was isolated from the cells using the Wizard® Plus Minipreps DNA Purification System or GeneJET Plasmid Miniprep kit (Thermo Fisher Scientific). To confirm assembly with double digestion, the plasmid DNA samples and corresponding vector backbones (5 µg) were incubated with restriction enzymes (Table 3) at 37 °C for at least 1 h. The plasmid DNA samples were compared to the vector control by 0.8-1% agarose gel electrophoresis. Colonies that had the correct digestion pattern were sent for confirmation via DNA sequencing using sequencing primers (Table 3, Genewiz).

Generally, confirmed plasmid DNA samples were transformed into *E. coli*

BL21(DE3) cells and plated on LB supplemented with the appropriate antibiotic. Confirmed plasmid DNA samples of pEA105/pEA106, however, were also transformed into *E. coli* BL21(DE3)Suf^{++} (PK11466, a kind gift of Dr. Patricia Kiley), which has enhanced levels of Suf machinery for [Fe-S] biogenesis, in order to increase *suf* expression and, subsequently, Grx3 protein expression, as Grx3 is a recombinant [Fe-S] cluster-containing protein.[9]

Table 3: Restriction enzymes used for double digestion and primers used for sequencing to confirm assembly of constructs.

Plasmid	Restriction Enzymes	Sequencing Primers
pEA100	*Hind*III *Sca*I-HF	T7 T7-Term
pEA102	*Eco*RV *Nru*I	DuetUP DuetDOWN1
pEA103/ **pEA104**	*Bsp*HI *Sac*I-HF	DuetUP2 T7-Term
pEA105/ **pEA106**	*Bsp*HI *Nco*I-HF	DuetUP1 T7-Term

Determination of Optimal Conditions for Small-Scale Overexpression

All small-scale overexpression trials were performed in 5-mL LB cultures grown at 37 °C with shaking and induced at OD_{600} 0.6 ~ 0.8. An aliquot of non-induced cells was harvested immediately before induction. For Aft1, cultures were induced with varying concentrations (0.25, 0.5, or 1 mM) of IPTG overnight at 30 °C or 0.25 mM IPTG for varying times (2, 4, or 6 h) at 30 °C. For Grx3/4 and Grx3/4-Bol2, cultures were induced with 0.25 mM IPTG for 4 h and overnight at 20 °C or 30 °C. One aliquot of the induced cells was harvested for all target proteins. For all targets except Grx3 and Grx3-Bol2, a second aliquot was treated with a bacterial protein extraction detergent (B-PER, Thermo Fisher Scientific) and centrifuged to extract the presumably soluble recombinant proteins from the cells and into the supernatant. Non-induced and induced cells and supernatant samples were resolved using sodium dodecyl sulfate polyacrylamide gel electrophoresis (SDS-PAGE).

Large-Scale Overexpression and Purification of Aft1 and Grx4

All large-scale overexpression trials were performed in 1 L LB cultures grown at 37 °C with shaking and induced with 1 mM IPTG or 0.5 mM IPTG at OD_{600} 0.6 ~ 0.8 for Aft1 or Grx4, respectively. For Aft1, the cultures were grown at 30 °C for 4 h. For Grx4, the cultures were grown at 30 °C for 18 h. Generally, an aliquot of non-induced cells was harvested prior to induction and the induced cells were collected via centrifugation at 6000 rpm for 10 - 20 min at 4 °C. The Aft1-containing cell pellets were washed with 30 mL of Lysis Buffer (50 mM Tris-HCl [pH 6.8], 500 mM NaCl, and 10 mM imidazole) before storage at -80 °C, while the Grx4-containing cell pellets were resuspended immediately before purification as described below. Once thawed and sonicated for purification, centrifugation of all cells was carried out at 16000 rpm for 40 min at 4 °C.

To purify Aft1, the pellet was thawed on ice for treatment with protease inhibitor. The cells were intermittently sonicated on ice for 3 min (30 s on and 60 s off) and centrifuged to obtain a cell-free supernatant. The supernatant was loaded onto a 5-mL HisTrap Nickel affinity column (Cytiva) equilibrated with 60 mL of Lysis Buffer. The column was washed with Lysis Buffer until no change was observed in the UV-visible absorption baseline reading. The protein was eluted in one step using 20 mL of Lysis Buffer with 500 mM imidazole, and the resulting fractions associated with a peak in UV-visible absorption readings were resolved with SDS-PAGE. The resulting bands of interest were cut and prepared for

mass spectrometry. Analysis of the mass spectrometry peaks was performed using the BLAST (Basic Local Alignment Search Tool) program with protein entries obtained from the NCBI database.

To purify Grx4, the pellet was thawed on ice, resuspended in 150 mL Buffer A (50 mM Tris-MES [pH 8.4], 1 mM GSH) with 180 µL phenyltmethanesulfonyl fluoride (PMSF), and treated with protease inhibitor. The cells were intermittently sonicated on ice for 12 min (15 s on and 45 s off) and centrifuged to obtain a cell-free supernatant. The supernatant was loaded onto a 20-mL diethylaminoethyl (DEAE) anion-exchange column (Cytiva) equilibrated with 80 mL of Buffer B (50 mM Tris-MES [pH 8.4], 1M NaCl,1 mM GSH) then 100 mL of Buffer A. The protein was eluted with a linear gradient from 0% - 100% Buffer B over 200 mL, and the resulting fractions associated with a peak in UV-visible absorption readings were resolved with SDS-PAGE.

Fluorescence Polarization with Aft1

The DNA binding ability of Aft1 was tested using a truncated form of Aft1 (Aft1(1-237)) that was cloned and purified by Evan Talib. This construct includes the DNA binding domain of Aft1 from amino acids 1-237 as well as the conserved CxC motif that is implicated in Fe-S binding. The affinity of this as-purified truncated Aft1 protein for the *FET3* iron-responsive element (FeRE) sequence in *C. glabrata* was tested using fluorescence polarization (FP). All FP measurements were performed on a Synergy H1 Hybrid Multi-Mode Reader (Biotek) in 96-well black polystyrene microplates (Corning) with 485 nm excitation and 528 nm emission filters. Calibration curves were run according to manufacturer recommendations with FP Buffer [50 mM Tris-HCl (pH 7.9), 150 mM NaCl, 1 mM TCEP, 1 mM EDTA], phosphate buffered saline (PBS), and sodium fluorescein to test the sensitivity and linearity of detection. An oligonucleotide corresponding to the region -748 to -717 in the *C. glabrata FET3* promoter that included the consensus iron response element (FeRE) sequence TGCACCC with a 6-carboxyfluorescein (6-FAM) fluorophore tag at the 5' end, and its untagged, reverse complement strand were ordered from Integrated DNA Technologies (IDT) (Table 4). The two complementary oligonucleotides (100 µM each mixed in a 1:1 molar ratio to achieve 50 µM final) were annealed by heating at 95 °C for 5 min and cooling to 25 °C over 45 min in a 5 °C stepwise gradient. The annealed oligonucleotides (50 µM doubled-stranded DNA) were confirmed with 3.5% agarose gel electrophoresis and diluted to 500 nM with FP Buffer. Generally, all dilutions of protein and DNA were made with FP Buffer for this assay.

Stock solutions of protein in varying concentrations (0.5, 1, 5, 10, 15, 20, and 40 µM) were prepared via serial dilution of 20 mg/mL as-purified Aft1(1-237). A stock solution of 10 nM ds-DNA was prepared via dilution of 500 nM ds-DNA. FP trials were run in triplicate with 120 µL reactions containing FP Buffer, 10 nM DNA, and increasing concentrations of protein in 32 wells.

Table 4: Oligonucleotides used for preparing fluorophore-labeled FeRE DNA. FeRE sequence highlighted in bold.

Oligo Name	Sequence
6FAM-Cgfet3-FeRE	5'- /6-FAM/CGC TTA TCG AAA A**TG CAC CC**A GGT GCC AAA CC -3'
RC-Cgfet3-FeRE	5'- GGT TTG GCA CCT **GGG TGC A**TT TTC GAT AAG CG-3'

For each reaction, the parallel intensity (I_{vv}) was read with both the excitation and emission polarizers vertically placed, and the perpendicular intensity (I_{vh}) was read with the excitation polarizer vertically placed and the emission polarizer horizontally placed. The grating factor (GF) for each reaction was calculated from the ratio of perpendicular and parallel intensities to correct for instrumental differences in sensitivity to emission intensities.[10] The fluorescence anisotropy (r) was calculated according to the following equation 1:[10]

$$\text{Eq. 1: } r = \frac{I_{vv} - (GF \times I_{vh})}{I_{vv} + (2 \times GF \times I_{vh})}$$

All fluorescence anisotropy values were normalized by subtracting the anisotropy value of DNA-buffer solution with no protein. This normalized change in anisotropy was plotted as a function of protein concentration and fit via nonlinear regression analysis to a one-site specific binding model using the algebraic curve fitting program GraphPad Prism as well as a single-site binding model using the numerical curve fitting program Dynafit.[11]

RESULTS AND DISCUSSION

Plasmid Construction

Amplification and Ligation of Insert

The target genes were amplified from *C. glabrata* genomic DNA using PCR. Agarose gel electrophoresis (Figure 1) shows bands at the expected sizes of 1651 bp for *AFT1*, 823 for *GRX4*, 297 bp for *BOL2*, and 779 bp for *GRX3* indicating that amplification of target genes was successful. PCR products were purified to isolate the gene of interest and resulting fragments were high quality DNA with little protein contamination as indicated by 260 nm/280 nm readings of 1.8 ~ 1.9. HA was utilized to ligate the target DNA inserts into the corresponding vector backbones forming

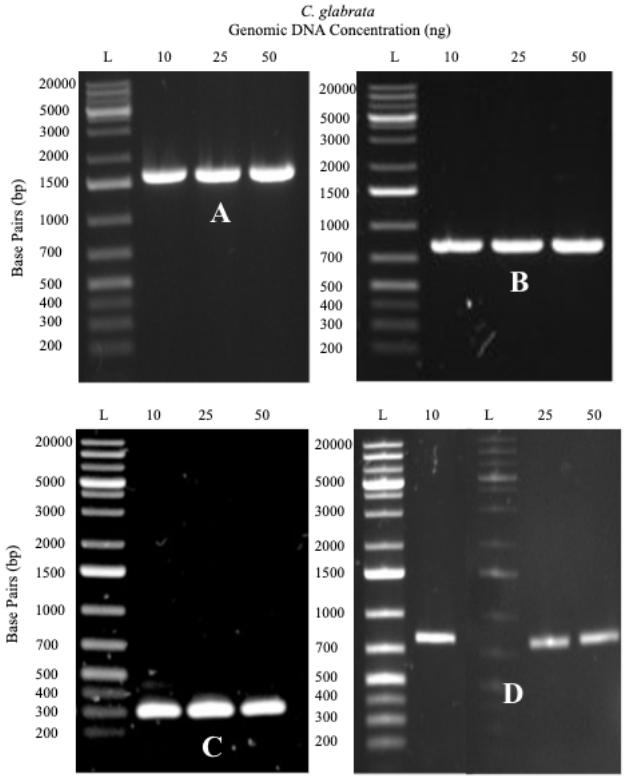

Figure 1: PCR amplification of *AFT1* (A), *GRX4* (B), *BOL2* (C), and *GRX3* (D) from *C. glabrata* genomic DNA. Agarose gel (0.8-1%) with 5-µL samples of PCR products from reactions containing 10 ng, 25 ng, and 50 ng *C. glabrata* genomic DNA. The first lane is a DNA ladder with fragments of known size indicated to the left.

expression plasmids for transformation into host cells. Successful incorporation of restriction enzyme sites into the sequence of interest and double digestion of vector backbones with the corresponding restriction enzymes (Table 1) allowed for ligation at the overlapping ends. Transformation of plasmids into *E. coli* DH5α resulted in amplification of recombinant DNA for miniprep isolation.

Confirmation of Assembly with Vector Backbones

Plasmid assembly was confirmed by double digestion with restriction enzymes (Table 3). Agarose gel electrophoresis for restriction digested pEA100 (Figure 2A) shows 2125-bp bands for all colonies indicating successful ligation of *AFT1* into the pET21a-6xHis vector; the pET21a-6xHis vector is missing the *AFT1* gene as indicated by the shorter 1080-bp band.

Agarose gel electrophoresis for restriction digested pEA102 (Figure 2B) shows 3192-bp bands for all colonies indicating successful ligation of *GRX4* into the pRSFDuet-1 vector; the pRSFDuet-1 vector is missing the *GRX4* gene as indicated by the shorter 2683-bp band.

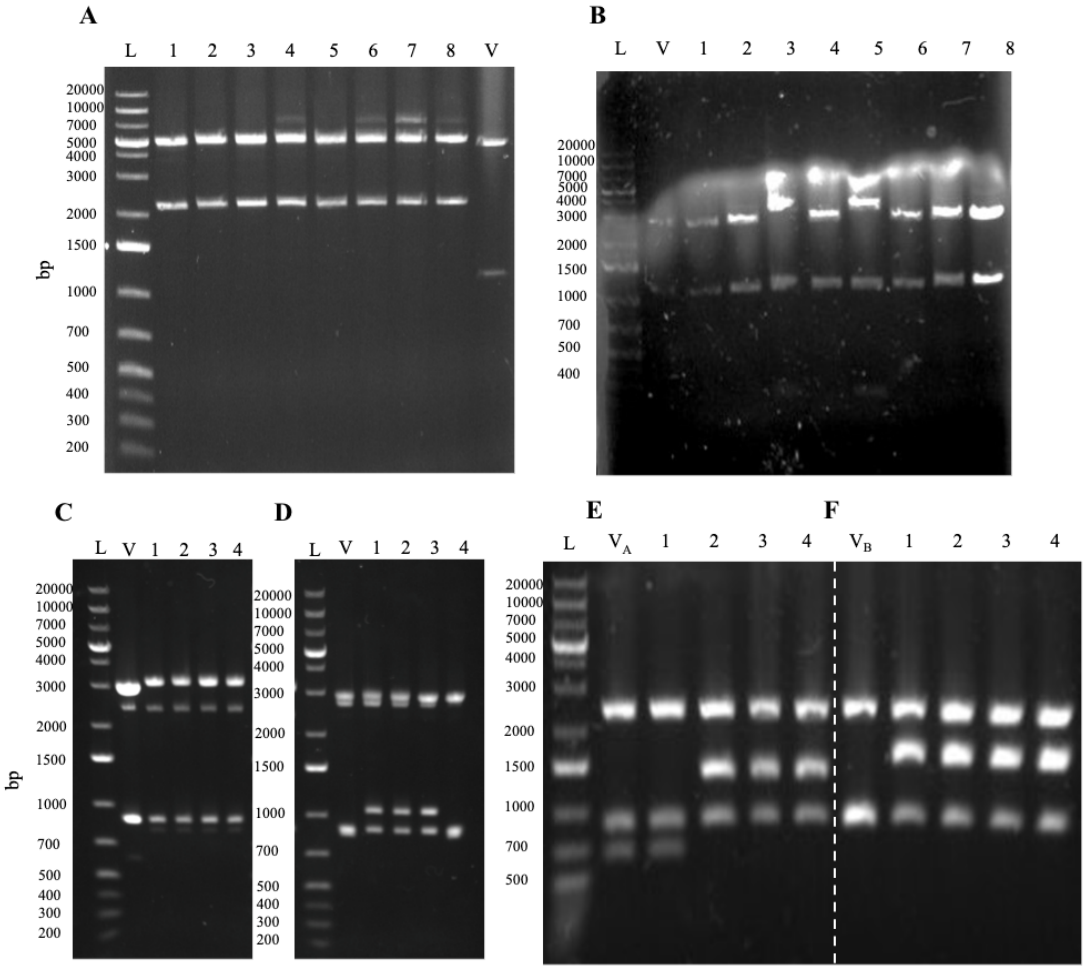

Figure 2: Double digestion with restriction enzymes for confirmation of pEA100 (A), pEA102 (B), pEA103 (C), pEA104 (D), pEA105 (E), and pEA106 (F). Agarose gel (0.8-1%) showing successful double digestion of the plasmids and their respective vector backbone as a control. V = pET21a (A), pRSFDuet-1 (B, C, E), pRSFDuet-1-Grx4 (D), and pRSFDuet-1-Bol2 (F). Numbers 1-8 indicate the colony from which plasmid DNA was isolated.

Agarose gel electrophoresis for restriction digested pEA103 (Figure 2C) shows 793-bp bands for all colonies indicating successful ligation of *BOL2* into the pRSFDuet-1 vector; the pRSFDuet-1 vector is missing the *BOL2* gene as indicated by the shorter 607-bp band. Agarose gel electrophoresis for restriction digested pEA104 (Figure 2D) shows 1031-bp bands for colonies 1-3 indicating successful ligation of *BOL2* into the pRSFDuet-1-Grx4 vector; the pRSFDuet-Grx4 vector is missing the *BOL2* gene as indicated by the shorter 845-bp band. The top bands (Figure 2) are undigested plasmid DNA further illustrating that the controls lack the *BOL2* insert and are shorter.

Agarose gel electrophoresis for restriction digested pEA105 (Figure 2E) shows 1354-bp bands for colonies 2-4 indicating successful ligation of *GRX3* into the pRSFDuet-1 vector; the pRSFDuet-1 vector is missing the *GRX3* gene as indicated by the shorter 656-bp band. Agarose gel electrophoresis for restriction digested pEA106 (Figure 2F) shows 1540-bp bands for all colonies indicating successful ligation of *GRX3* into the pRSFDuet-1-Bol2 vector; the pRSFDuet-Bol2 vector is missing the *GRX3* gene as indicated by the shorter 842-bp band.

Colonies that appeared correct for each construct were confirmed by DNA sequencing (Table 3) before transformation into *E. coli* strain BL21(DE3) or BL21(DE3)Suf^{++} for protein expression.

Determination of Optimal Conditions for Small-Scale Overexpression

Small-scale cultures inoculated with pEA100 in the *E. coli* BL21(DE3) host strain were induced with 0.25, 0.5, or 1 mM of IPTG overnight at 30 °C or 37 °C as well as 0.25 mM IPTG for 2, 4, or 6 h at 30 °C or 37 °C. The expected MW of Aft1 is 61 kD; however, on our gels Aft1 has consistently run at ~71 kD (Figure 3). This anomalous migration may be due to post-translational modifications of the protein or acidic residues that interfere in SDS binding during SDS-PAGE. Regardless of this slow migration tendency, the expression pattern between non-induced and induced conditions strongly suggested that this was the correct band, and mass spectrometry confirmed this.

SDS-PAGE gel electrophoresis (Figure 3A) depicts a band at ~71 kD in induced samples that is absent in non-induced samples indicating that Aft1 was successfully expressed after induction with 0.25, 0.5, or 1 mM IPTG and growth for 18 h at 30 °C or 37 °C. The 71-kD bands in supernatant samples confirm that Aft1 is a soluble protein, as it was successfully extracted from the cells during B-PER treatment. This applies to the respective bands and solubility of Grx3/4 and Bol2 as well. The faint bands in the non-induced samples around the expected molecular weight for Aft1 are not concerning due to the presence of native *E. coli* proteins and the clear difference between this faint band and the sharper band that appears only in the induced sample. The sharpest and most intense 71-kD bands in Figure 3A appeared after growth at 30 °C (left) rather than 37 °C (right). Thus, we relied on the 30 °C growth condition for determining the optimal concentration of IPTG for induction. The 71-kD induced band for 0.25 mM IPTG and growth at 30 °C (Figure 3A) appears slightly sharper and more intense than the other bands of interest supporting that overexpression of Aft1 with varied inducing agent concentration was optimized by induction with 0.25 mM IPTG.

This optimal concentration of inducing agent was held constant as induction time was varied. SDS-PAGE gel electrophoresis (Figure 3B) depicts a band at ~71 kD in induced samples that is absent in non-induced samples indicating that Aft1

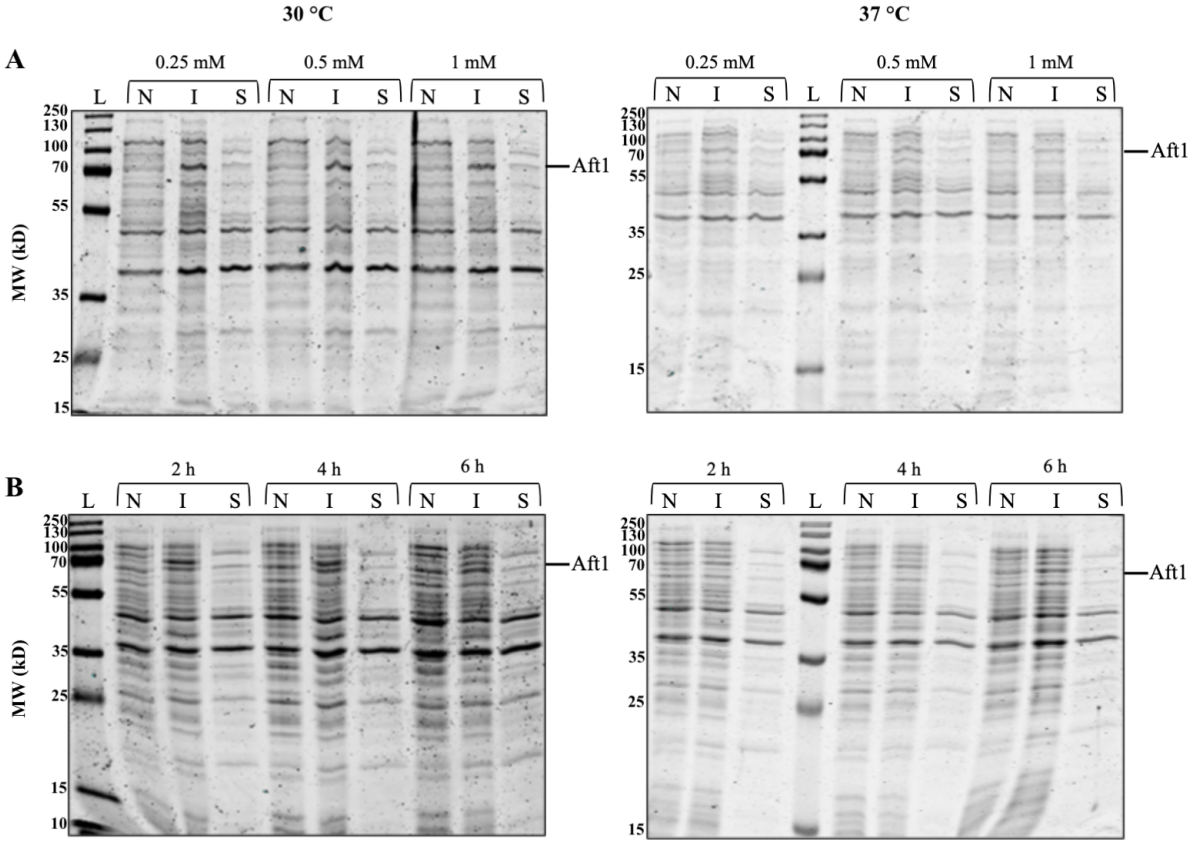

Figure 3: Expression of recombinant Aft1 (expected MW = 61 kD). (A) SDS-PAGE gels comparing Aft1 protein expression after induction with three IPTG concentrations and overnight growth at two temperatures. (B) SDS-PAGE gels comparing Aft1 protein expression after induction with 0.25 mM IPTG and three growth intervals at two temperatures. The sizes of the molecular weight ladder standards (MW; kD) are listed to the left of each gel. L = ladder, N = non-induced cells, I = induced cells, and S = supernatant.

was successfully expressed after induction with 0.25 mM IPTG and growth for 2, 4, or 6 h at 30 °C or 37 °C. Again, the sharpest and most intense 71-kD induced bands in Figure 3B appeared after growth at 30 °C (left) rather than 37 °C (right) further supporting the conclusion that the lower temperature is more favorable for expression of Aft1. The 71-kD induced band for 4-h growth at 30 °C (Figure 3B) appears slightly sharper and more intense than the other bands of interest supporting that overexpression of Aft1 with varied induction times was optimized by growth for 4 h. These findings support the conclusion that the optimal conditions tested for Aft1 overexpression were induction with 0.25 mM IPTG followed by growth for 4 h at 30 °C.

The optimization of Aft1 expression after growth at 30 °C supports the finding that growth at 30 °C rather than the optimal *E. coli* growth temperature (37 °C) may be beneficial for the expression of soluble proteins in pET Vector Systems by avoiding accumulation as inclusion bodies.[12,13] Growth at 20 °C and accommodating with overnight incubation has been also been recommended for soluble protein expression.[12,13] While protein degradation during the overnight condition is possible, these suggested conditions of lower temperature and prolonged growth may allow for better

folding of soluble proteins and have been utilized for successful expression of recombinant Aft2, Bol2, and Grx3/4 from *S. cerevisiae.*[4-6,12-14]

Based on the optimal conditions found by our lab during expression studies of Aft1 from *C. glabrata*, induction with 0.25 mM IPTG for 4 h at 30 °C were growth parameters of interest for optimizing overexpression of Grx3/4 and Bol2 from *C. glabrata*. Based on recommendations for growth at 20 °C and overnight incubation,[12,13] these growth parameters were also tested for optimizing overexpression of these potential binding partners. As such, small-scale cultures inoculated with pEA102-106 in the *E. coli* BL21(DE3) host strain were induced with 0.25 mM IPTG and grown for 4 h or overnight at 20 °C or 30 °C.

SDS-PAGE gel electrophoresis (Figure 4) depicts a band at ~27 kD in induced samples that is absent in non-induced samples indicating that Grx4 was successfully expressed after induction with 0.25 mM IPTG. The sharpest and most intense 27-kD induced bands in Figure 4 appeared after 4-h growth (left) rather than 18-h growth (right). The 27-kD induced band for 4 h of growth at 30 °C (Figure 4) appears sharper and more intense than the other bands of interest supporting that the optimal expression conditions tested for Grx4 were induction with 0.25 mM IPTG followed by growth for 4 h at 30 °C.

The expected MW of Bol2 is 9.5 kD; however, on our gels Bol2 has consistently run at ~11 kD (Figure 5). As with Aft1, this anomalous migration may be due to post-translational modifications of the protein or acidic residues that interfere in SDS binding during SDS-PAGE. Of note, Bol2 orthologs from other organisms also run at a higher MW than expected.[5,6] Protein mass spectrometry and size exclusion chromatography will be used in the future to assess the size of Bol2 from *C. glabrata* more accurately.

SDS-PAGE gel electrophoresis (Figure 5) depicts a band at ~11 kD in induced samples that is absent in non-induced samples indicating that Bol2 was successfully expressed after induction with IPTG both alone and in the presence of Grx4. SDS-PAGE gel electrophoresis (Figure 5B) depicts a band at ~26 kD that is unique to the induced samples for the complexed construct

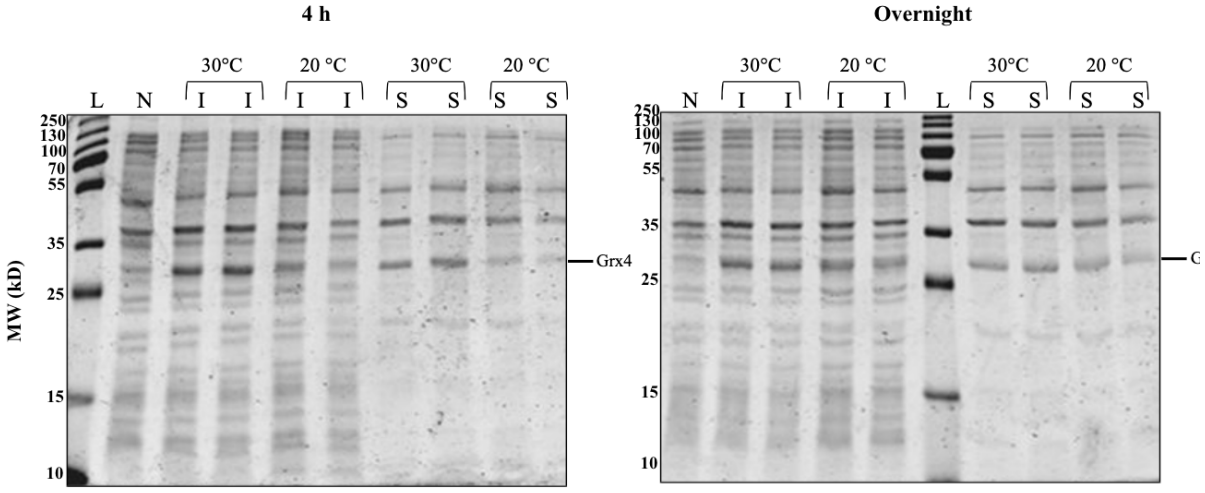

Figure 4: Expression of recombinant Grx4 (expected MW = 29.8 kD). SDS-PAGE gels comparing Grx4 protein expression after induction with 0.25 mM IPTG and growth for two intervals at two temperatures. The sizes of the molecular weight ladder standards (MW; kD) are listed to the left of each gel. L = ladder, N = non-induced cells, I = induced cells, and S = supernatant.

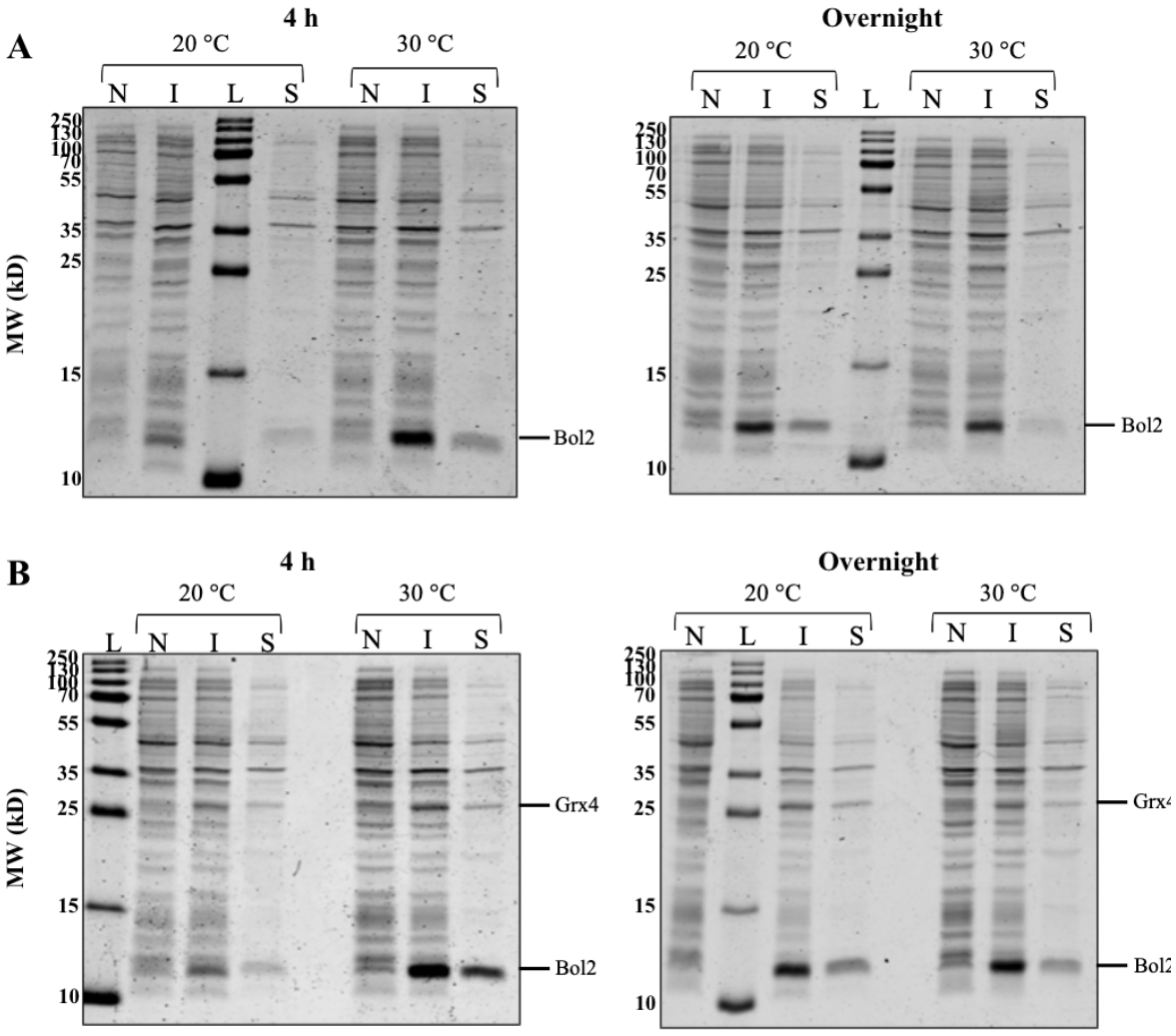

Figure 5: (A) Expression of recombinant Bol2 (expected MW = 9.5 kD). SDS-PAGE gels comparing Bol2 protein expression after induction with 0.25 mM IPTG and growth for two intervals at two temperatures. (B) Co-expression of Bol2 and Grx4 (expected MW = 29.8 kD). SDS-PAGE gels comparing Bol2 and Grx4 co-expression with same induction and growth conditions as (A). The sizes of the molecular weight ladder standards (MW; kD) are listed to the left of each gel. L = ladder, N = non-induced cells, I = induced cells, and S = supernatant.

and absent in non-induced samples indicating that Grx4 was successfully expressed in the presence of Bol2 after induction with IPTG. The 11-kD induced band for 4 h of growth at 30 °C (Figure 5A) appears sharper and more intense than the other bands of interest supporting that the optimal expression conditions tested for Bol2 alone were induction with 0.25 mM IPTG followed by growth for 4 h at 30 °C. The 11-kD and 26-kD induced bands for 4 h of growth at 30 °C (Figure 5B) both appear sharper and more intense than the other bands of interest indicating that the optimal conditions tested for Bol2 and Grx4 co-expression were also induction with 0.25 mM IPTG followed by growth for 4 h at 30 °C. The intensity of the 11-kD band (Figure 5) is consistent for Bol2 alone and in the presence of Grx4 suggesting that Grx4 co-expression does not hinder Bol2 expression.

Grx3 expression in *E. coli* BL21(DE3) was faint and difficult to discern (data not shown, E. Talib, C. Outten lab unpublished data), so Grx3 expression in *E. coli* BL21(DE3)Suf^{++} (PK11466) was tested. SDS-PAGE gel electrophoresis (Figure 6) depicts a band at ~26 kD in induced samples that is absent in non-induced samples indicating that Grx3 was successfully expressed after induction with IPTG both alone and in the presence of Bol2. SDS-PAGE gel electrophoresis (Figure 6B) depicts a band at ~11 kD that is unique to the induced samples for the complexed construct and absent in non-induced samples indicating that Bol2 was successfully expressed in the presence of Grx3 after induction with IPTG. The 26-kD induced band for overnight growth at 30 °C (Figure 6A) appears sharper and more intense than the other bands of

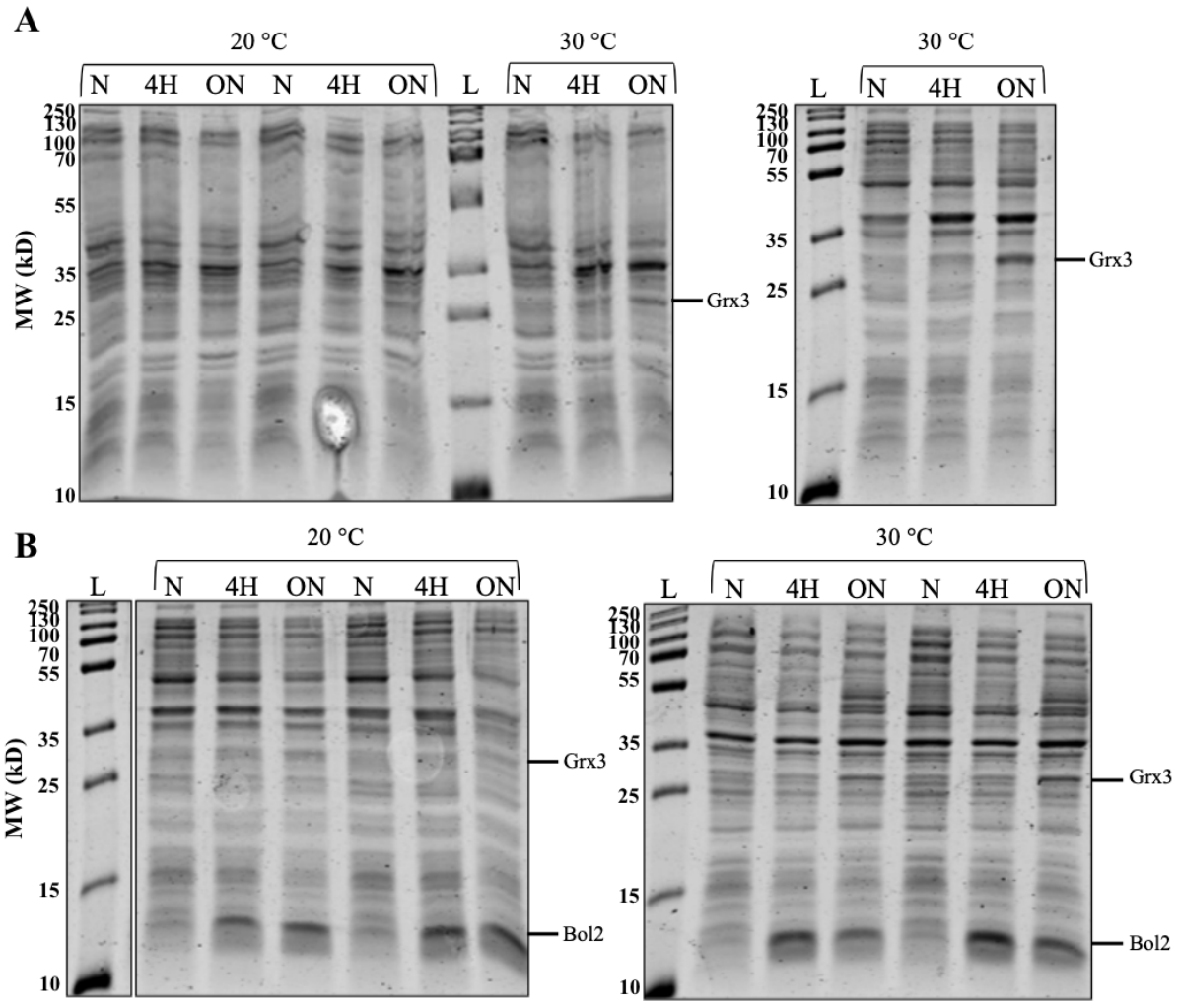

Figure 6: (A) Expression of recombinant Grx3 (expected MW = 27.5 kD). SDS-PAGE gels comparing Grx3 protein expression after induction with 0.25 mM IPTG and growth for two intervals at two temperatures. (B) Co-expression of Grx3 and Bol2 (expected MW = 9.5 kD). SDS-PAGE gels comparing Grx3 and Bol2 co-expression with the same growth conditions as (A). The sizes of the molecular weight ladder standards (MW; kD) are listed to the left of each gel. L = ladder, N = non-induced cells, 4H = 4 hours induced cells, ON = overnight induced cells.

interest supporting that the optimal expression conditions tested for Grx3 alone were induction with 0.25 mM IPTG followed by overnight growth at 30 °C.

For Grx3 and Bol2 co-expression, the 26-kD induced bands for overnight growth at 30 °C are also stronger than the other 26-kD bands of interest, but the 11-kD induced bands for 4-h growth at 30 °C rather than overnight growth appear stronger than the other 11-kD bands of interest (Figure 6B). This intensity inversion for the 11-kD and 26-kD bands (Figure 6B) between 4 h and overnight conditions, which is seen for Grx3-Bol2 but not Grx4-Bol2, suggests that co-expression with Grx3 may hinder Bol2 expression. The optimal expression conditions tested for Grx3-Bol2 appear to be the same as for Grx3, namely0.25 mM IPTG followed by overnight incubation at 30 °C, to ensure that Grx3 overexpression is also achieved.

Large-Scale Overexpression and Purification of Aft1 and Grx4

The protein fractions obtained by purifying Aft1 via affinity chromatography on a HisTrap Nickel column were expected to contain a 71-kD band if expression and purification were successful; the bands marked in Figure 7 appear to be the Aft1 band.

The cell lysate, supernatant, pellet, wash, and flow-through samples analyzed were collected at separate steps during the purification protocol. The cell lysate sample was collected after sonication of cells prior to centrifugation. The supernatant and pellet samples were collected after separation via centrifugation. The remaining supernatant was loaded on the HisTrap Nickel column, and a sample was collected after washing with Lysis Buffer to determine if protein had been prematurely removed from the column. Due to the C-terminal 6xHis tag on Aft1, the protein was expected to bind the nickel resin in the column until imidazole competition was introduced. Fractions 10-22 were collected after one-step elution with 500 nM imidazole and pooled for concentration.

This 71-kD band of interest and the thinner band below it for protein fraction 15 were isolated and sent for mass spectrometry analysis. The thick 35-kD and 20-kD bands, which were expected to be native *E. coli* proteins, were also sent for analysis. Mass spectrometry and subsequent BLAST analysis demonstrated that Aft1-6xHis was the protein that appeared at 71 kD and that *E. coli* proteins did, in fact, appear at 35 kD and 20 kD. Furthermore, the thin band directly below the 71-kD band was the Aft1-6xHis protein with slight degradation. This protein purification on HisTrap column will be

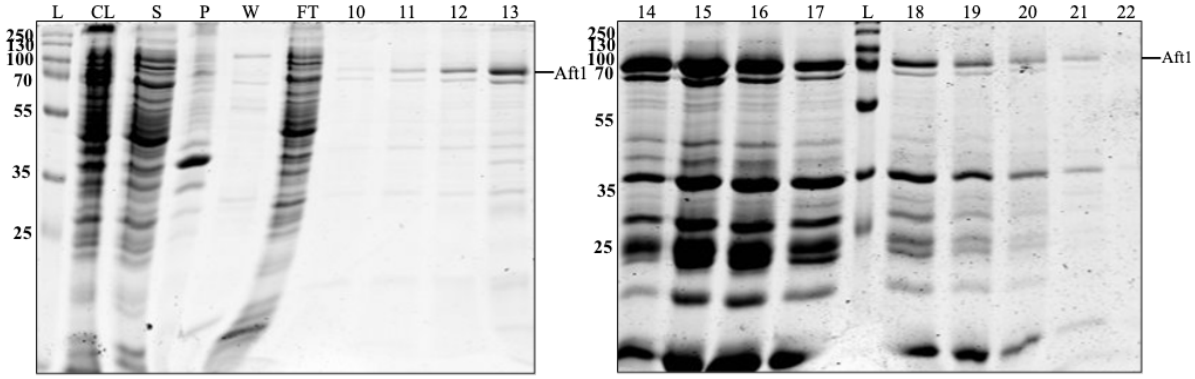

Figure 7: Purification of Aft1 on HisTrap Nickel column. The sizes of the molecular weight ladder standards (MW; kD) are listed to the left of each gel. L = ladder, CL = cell lysate, S = supernatant, P = pellet, W = wash, FT = flow-through, 10-22 = protein fractions collected.

repeated on a Heparin column in hopes of improving the purification strategy.

The protein fractions obtained by purifying Grx4 via anion-exchange chromatography on a DEAE column were expected to contain a 27-kD band if expression and purification were successful; the bands marked in Figure 8 appear to be the Grx4 band. The pellet, supernatant, and flow-through samples analyzed were collected at separate steps during the purification protocol. Due to the net negative charge of Grx4 in Buffer A, the protein was expected to bind to the positively charged DEAE column until chloride anion competition from Buffer B was introduced. Fractions 27-35 were collected after elution with a Buffer B gradient and pooled for concentration. We will confirm the identity of these bands (Figure 8) with mass spectrometry and subsequent BLAST analysis.

In the future, we will scale up the optimized conditions for small-scale expression to large-scale expression studies for Grx3 and Bol2 from *C. glabrata*. We will also purify Grx3 and Bol2 following the protocol previously described for the *S. cerevisiae* homologs.[5]

Fluorescence Polarization with Aft1

Fluorescence polarization involves exciting a biological macromolecule in solution with vertically polarized light and measuring the emission of vertically polarized and horizontally polarized light to obtain the parallel and perpendicular intensities, respectively, which determine anisotropy values (Eq. 1).[10, 15] Fluorophores that tumble slowly in solution will have differential parallel and perpendicular intensities and high anisotropy values; those that tumble quickly will have similar intensities and low anisotropy values.[15] As protein binds fluorescently-labeled DNA, the mass is expected to increase causing the tumbling rate to decrease which suggests that protein-DNA binding can be detected by changes in anisotropy.[15]

In *S. cerevisiae*, Aft1 binds the promoter region of target genes containing the consensus FeRE sequence, TGCACCC, to activate their transcription in iron deplete conditions.[3,4] One of these target genes is *FET3* which encodes a multicopper oxidase that functions with the Ftr1 iron permease to import ionic iron into the cell.[3] The regulatory functions of Aft1 and the promoter sequence of *FET3* are well conserved between *S. cerevisiae* and *C. glabrata* so we assume that *C. glabrata* Aft1 recognizes a similar FeRE in the promoter of *FET3*. The DNA-binding affinity of as-purified Aft1(1-237) for the *FET3* promoter in *C. glabrata* was analyzed in triplicate via a fluorescence

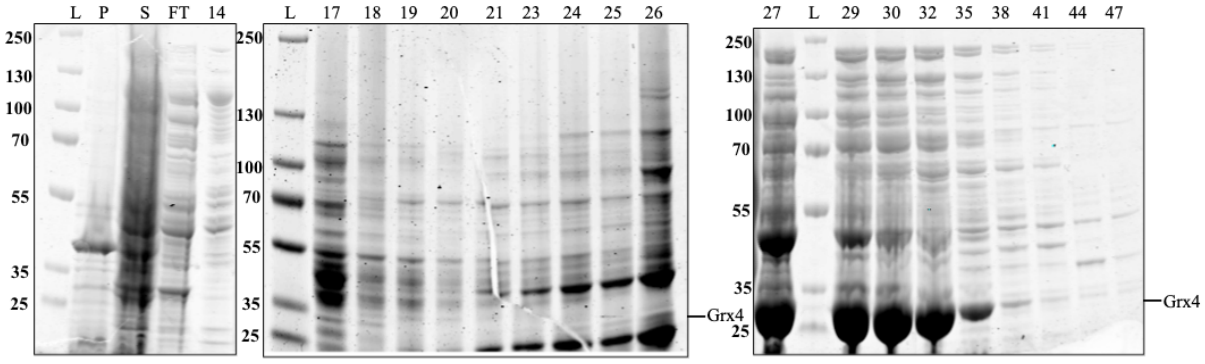

Figure 8: Purification of Grx4 on DEAE column. The sizes of the molecular weight ladder standards (MW; kD) are listed to the left of each gel. L = ladder, P = pellet, S = supernatant, FT = flow-through, 14-47 = protein fractions collected.

polarization assay. The DNA dissociation constant of *C. glabrata* Aft1(1-237) was found to be 280 ± 160 nm, 800 ± 140 nM, and 730 ± 170 nM from the Dynafit model (Figure 9). These results clearly demonstrate for the first time that *C. glabrata* Aft1(1-237) specifically binds the FeRE of *FET3* with high nanomolar affinity. Though the results were similar between the two models, the Dynafit program may be beneficial for analyzing our Aft1-FeRE DNA binding interactions in general, as it is applicable to more experimental conditions than the Prism model which assumes that the DNA concentration is 100X less than the protein dissociation constant.[11]

The Aft2 homolog from *S. cerevisiae* has a published DNA dissociation constant of 26.1 ± 3.3 nM so we expected a similar binding affinity for *C. glabrata* Aft1.[4] Our unexpectedly high dissociation constants determined for *C. glabrata* Aft1(1-237) may be due to inaccurate protein concentrations from the Bradford assay, an insufficient zinc load on Aft1 preventing DNA binding, or the binding reactions not reaching equilibrium. Improved calibration of the Bradford assay for Aft1(1-237), characterization of zinc-binding of the protein, and manipulation of reaction incubation time may be beneficial to optimize future fluorescence polarization assays. Nevertheless, these results successfully demonstrate that *C. glabrata* Aft1 specifically recognizes the putative FeRE in the *FET3* promoter.

CONCLUSION

Our results show that the primary iron-responsive transcription factor Aft1, the monothiol glutaredoxins Grx3 and Grx4, and the BolA-like protein Bol2 from *C. glabrata* were successfully cloned and recombinantly overexpressed in *E. coli*. As potential binding complexes of Aft1, Grx3/4 and Bol2 were

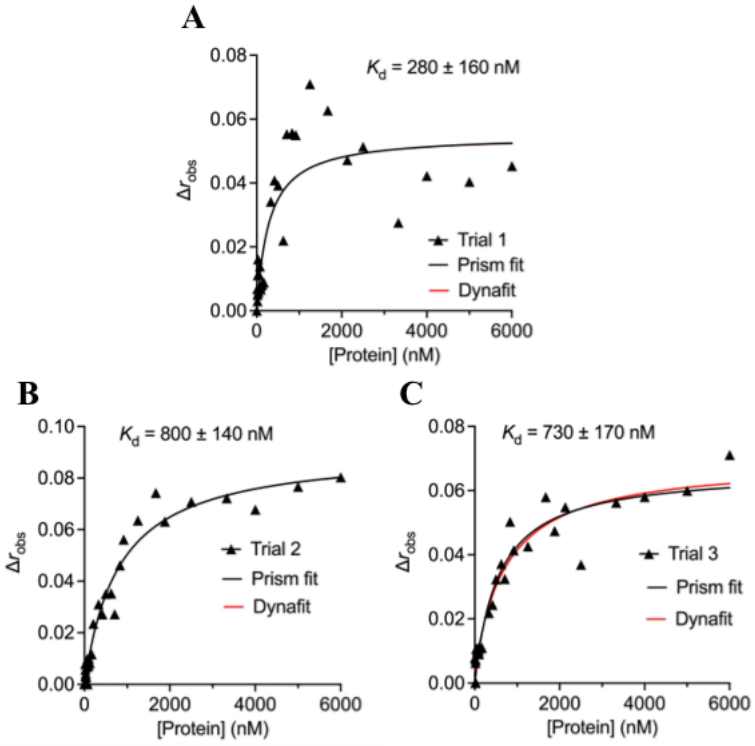

Figure 9: Binding of Aft1(1-237) to 6-FAM-labeled *FET3* promoter DNA for Trial 1 (A), Trial 2 (B), and Trial 3 (C). The triangles indicate changes in normalized anisotropy (Δr_{obs}). The solid lines depict nonlinear regression fits using Prism (black) or Dynafit (red). K_d = Dissociation constant

overexpressed both alone and in complex. The optimal conditions for overexpression of Aft1, Grx4, Bol2, and Grx4-Bol2 in complex were found to be induction with 0.25 mM IPTG followed by incubation for 4 h at 30 °C. The optimal conditions for overexpression of Grx3, however, differed by incubation time, as they were found to be induction with 0.25 mM IPTG followed by overnight incubation at 30 °C. While co-overexpression of Bol2 with Grx3 was optimized by the same conditions as overexpression of Bol2 alone, overexpression of Grx3 in this complex was not favored by these conditions. Thus, the optimal conditions for overexpression of Grx3-Bol2 were found to be the same as Grx3 alone, namely 0.25 mM IPTG followed by overnight incubation at 30 °C.

The overexpression conditions identified here were used on a larger scale to overexpress and purify Aft1 and Grx4. A fluorescence polarization assay was used to monitor Aft1-DNA binding with as-purified Aft1(1-237) from *C. glabrata* and *FET3* promoter DNA. The DNA dissociation constant of as-purified Aft1(1-237) was found to be 280 ± 160 nm, 800 ± 140 nM, and 730 ± 170 nM through triplicate analysis. These values were higher than those published for the Aft2 homolog in *S. cerevisiae* indicating that this assay should be repeated to obtain more accurate values.[4]

Bol2 and Grx3 will need to be purified for use in future interaction studies of these binding partners and the iron-responsive transcription factor Aft1 from *C. glabrata*. UV-visible absorption, circular dichroism, and electron paramagnetic resonance spectroscopies will be utilized to study the Fe-S cluster binding characteristics of Grx3/4 and Bol2 in the presence or absence of Aft1. Furthermore, the impact apo and Fe-S cluster-bound Grx3/4 and Bol2 on the DNA binding activity of Aft1 will be measured to test the post-translational mechanism for regulating Aft1 activity in response to iron. Delineating these characteristics will further elucidate the role of Fe-S clusters in iron regulation in *C. glabrata* and indicate how regulation in this fungal pathogen compares to that of the non-pathogenic yeast *S. cerevisiae*.

REFERENCES

1. Wallace DF (2016) The regulation of iron absorption and homeostasis. *Clin Biochem Rev* 37(2):51-62.
2. Himmelfarb J (2007) Iron regulation. *JASN* 18(2):379-381.
3. Devaux F, Thiébaut A (2019) The regulation of iron homeostasis in the fungal human pathogen Candida glabrata. *Microbiology* 165(10):1041-1060.
4. Poor CB, Wegner SV, Li H, Dlouhy AC, Scheurmann JP, Sanishvili R, Hinshaw JR, Riggs-Gelasco PJ, Outten CE, He C (2014) Molecular mechanism and structure of the *Saccharomyces cerevisiae* iron regulator Aft2. *PNAS* 111(11):4043-4048.
5. Li H, Mapolelo DT, Dingra NN, Naik SG, Lees NS, Hoffman BM, Riggs-Gelasco PJ, Huynh BH, Johnson MK, and Outten CE (2009) The yeast iron regulatory proteins Grx3/4 and Fra2 form heterodimeric complexes containing a [2Fe-2S] cluster with cysteinyl and histidyl ligation. *Biochemistry* 48(40):9569-9581.
6. Li H, Mapolelo DT, Dingra NN, Keller G, Riggs-Gelasco PJ, Winge DR, Johnson MK, Outten CE (2011) Histidine 103 in Fra2 is an iron-sulfur cluster ligand in the [2Fe-2S] Fra2-Grx3 complex and is required for *in vivo* iron signaling in yeast. *J Biol Chem* 286(1):867-876.
7. Ojeda L, Keller G, Mühlenhoff U, Rutherford JC, Lill R, Winge DR (2006) Role of glutaredoxin-3 and glutaredoxin-4 in the iron regulation of the Aft1

transcriptional activator in *Saccharomyces cerevisiae*. *J Biol Chem* 281(26):17661-17669.
8. Gerwien F, Safyan A, Wisgott S, Hille F, Kaemmer P, Linde J, Brunke S, Kasper L, Hube B (2016) A novel hybrid iron regulation network combines features from pathogenic and nonpathogenic yeasts. *ASM* 7(5):1-16.
9. Corless EI, Mettert EL, Kiley PJ, Antony, E (2019) Elevated expression of a functional Suf pathway in *Escherichia coli* BL21(DE3) enhances recombinant production of an iron-sulfur cluster-containing protein. *J Bacteriol* 202(3):e00496-19.
10. Favicchio R, Dragan AI, Kneale GG, Read CM (2009) Fluorescence spectroscopy and anisotropy in the analysis of DNA-protein interactions. Methods Mol Biol 543:589-611.
11. Kuzmic P (1996) Program DYNAFIT for the analysis of enzyme kinetic data: application to HIV proteinase. *Anal Biochem*. 237(2):260-273.
12. Novagen, Inc. (1999) pET system manual. United States and Canada. TB055 8th Edition 02/99. 8th ed. Available from: https://research.fredhutch.org/content/dam/stripe/hahn/methods/biochem/pet.pdf .
13. Novagen, Inc. (2006) pET system manual. United States and Canada. TB055 11th Edition 01/06. 11th ed. Available from: http://kirschner.med.harvard.edu/files/protocols/Novagen_petsystem.pdf .
14. Li H, Outten CE (2019) The conserved CDC motif in the yeast iron regulator Aft2 mediates iron–sulfur cluster exchange and protein–protein interactions with Grx3 and Bol2. *J Biol Inorg.* 48(40):9569-9581
15. Anderson BJ, Larkin C, Guja K, Schildbach JF (2008) Using fluorophore-labeled oligonucleotides to measure affinities of protein-DNA interactions. *Methods Enzymol*. 450:253-272.